

Active slip control of a vehicle using fuzzy control and active suspension

Muhammad Arshad Khan, Saima Haroon, Ejaz Ahmad, Bashir Hayat & Iljoong Youn

To cite this article: Muhammad Arshad Khan, Saima Haroon, Ejaz Ahmad, Bashir Hayat & Iljoong Youn (2021) Active slip control of a vehicle using fuzzy control and active suspension, *Automatika*, 62:3-4, 386-396, DOI: [10.1080/00051144.2021.1972399](https://doi.org/10.1080/00051144.2021.1972399)

To link to this article: <https://doi.org/10.1080/00051144.2021.1972399>



© 2021 The Author(s). Published by Informa UK Limited, trading as Taylor & Francis Group.



Published online: 02 Sep 2021.



Submit your article to this journal [↗](#)



Article views: 457



View related articles [↗](#)



View Crossmark data [↗](#)



Active slip control of a vehicle using fuzzy control and active suspension

Muhammad Arshad Khan^a, Saima Haroon^b, Ejaz Ahmad^a, Bashir Hayat^c and Iljoong Youn^a

^aSchool of Mechanical and Aerospace Engineering, ReCAPT, Gyeongsang National University, Jinju, South Korea; ^bDepartment of Computer Science, King Khalid University Abha, , Kingdom of Saudi Arabia; ^cDepartment of Informatics, Gyeongsang National University, Jinju, South Korea

ABSTRACT

This paper presents an active slip control system (ASCS) for a four-wheel drive electric vehicle (EV) using an active suspension of the vehicle. The integrated control mechanism is designed using a combination of a fuzzy controller and a nonlinear back-stepping controller to control the slip of the individual wheels with the help of the active suspension of the vehicle. In this research, the presented control mechanism is implemented in two steps. In the first step, based on the friction coefficient calculated from a nonlinear tire model, the fuzzy controller will generate the vehicle roll and pitch angles required to reduce the slipping of the individual wheels by changing the vertical load of the individual wheel. In the second step, a nonlinear back-stepping controller is used to track the required roll and pitch angles using the active suspension of the vehicle. A linear seven degree of freedom (DOF) vertical mathematical model is used for the design of the nonlinear back-stepping controller, while the rules of the fuzzy controller are interpreted from the friction coefficients of the tyre model. The performance of the presented control mechanism is verified using a 14-DOF nonlinear model with nonlinear tyre dynamics. The simulations using a nonlinear vehicle model show that the presented controller can successfully improve vehicle stability by reducing the slipping of the individual wheel.

ARTICLE HISTORY

Received 12 March 2020
Accepted 10 August 2021

KEYWORDS

Fuzzy control; active slip control; nonlinear control; active suspension; electric vehicle

1. Introduction

Recent years have witnessed an increasing demand for electric vehicle (EV). Due to the development of the advance technology for safety and high mobility the environment friendly EV has become a prime focus of research in the automobile industry [1]. With the introduction of in-wheel motors, the four independent wheel drive (4IWD) vehicles with four independent electric motors are considered to be more easily controllable as compared to the internal combustion engine vehicles [2]. The emergence of the independently actuated (IA) drive in EV opened many new research areas for the improvement of the manoeuvrability and active safety [3–6].

In spite of the fact that four independent in-wheel motors can result in fast and accurate torque distribution for the motion control of the vehicle, controlling such a vehicle, especially in corners and slippery conditions, is a most challenging task for the control designers [7,8].

Different control techniques are utilized to prevent the vehicle from driving out of its desired path [9]; to name few, for electronic stability controller (ESC), see [10,11], many studies were conducted regarding vehicle chassis attitude control [12,13] and integrated full-vehicle active safety control systems, see [14–16]. Although the above-mentioned techniques

greatly improve the performance of the vehicle in normal and some extreme conditions but the slipping of tyres always limit the performance of the mentioned techniques. The friction forces between the road and tyres are normally defined by the road conditions and are usually out of control of vehicle driver, and the performance of all active chases control techniques mainly depends on the tyre friction forces.

Active suspension systems have been widely studied for the improvement of the attitude control where the main task is to improve the ride comfort of the vehicle by using the suspension deflection of the individual wheels to reduce the roll, pitch and heave motions of chassis during different road disturbances, especially in sharp corners and braking manoeuvres [17–19].

This work is aimed at using active suspension of the vehicle to reduce slipping of the individual wheels. The basic idea behind the need for an active slip control system (ASCS) is the loss of road grip that can lead to poor steering control and loss of stability of vehicles because of the difference in tyre forces of the vehicle wheels. In this paper, with the help of suspension deflection the vertical load of the individual wheels is manipulated in such a way that improves the slipping of the wheels. The presented integrated control mechanism is designed using a combination of a fuzzy controller

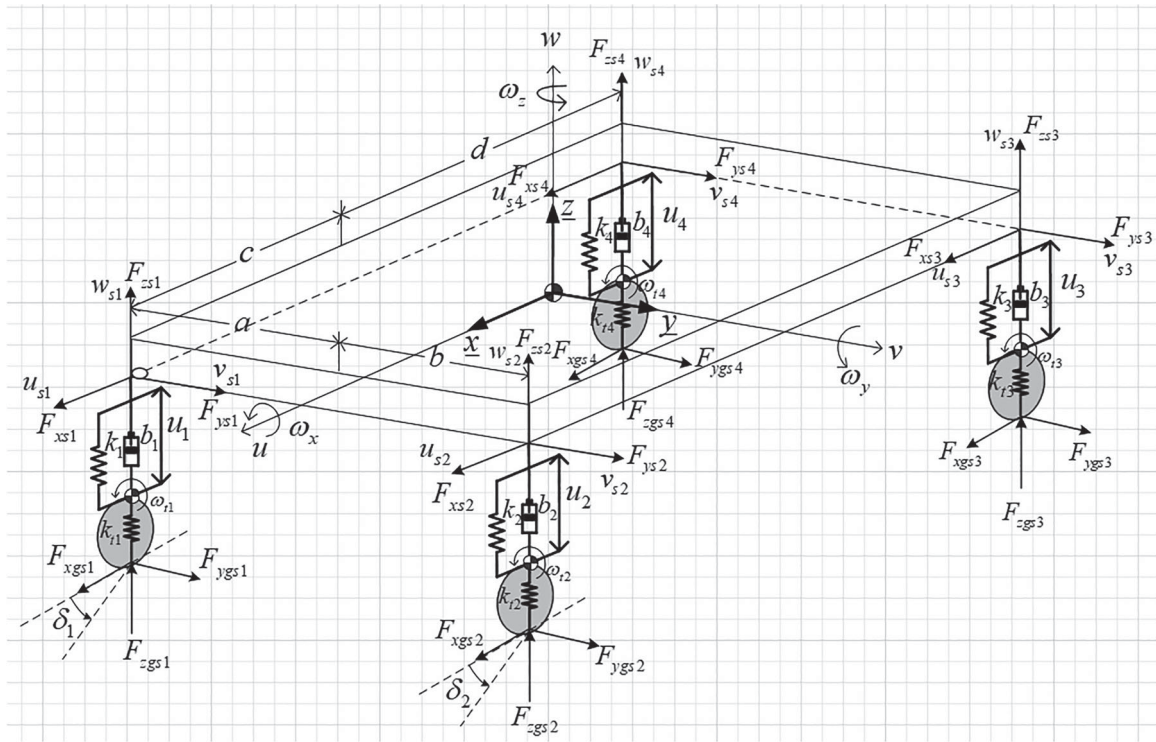


Figure 1. 14-DOF non-linear vehicle model.

and a nonlinear back-stepping controller to control the slip of the individual wheels with the help of the active suspension of the vehicle.

In this research, the presented control mechanism is implemented in two steps. In the first step, based on the friction coefficient calculated from a nonlinear tire model, the fuzzy controller will generate the required pitch and roll angle needed to reduce the slipping by changing the vertical load of the individual wheel, in the second step a nonlinear back-stepping controller is used to track the desired pitch and roll angle using the active suspension of the vehicle.

A linear seven degree of freedom (DOF) vertical mathematical model is used for the design of the nonlinear back-stepping controller, while the rules of the fuzzy controller are interpreted from the friction coefficients of the tyre model. The performance of the presented control mechanism is verified using a 14-DOF nonlinear model with nonlinear tyre dynamics. The simulations using a nonlinear vehicle model under different driving conditions show that the presented controller can successfully improve vehicle stability by reducing the slipping of the individual wheel.

The rest of this paper is organized as follows. Section 2 presents the mathematical models of the tyre and vehicle. Section 3 describes the design procedure for the integrated controller. Simulation results using a high fidelity nonlinear vehicle model are discussed in Section 4, followed by conclusion.

2. Vehicle mathematical model

This section explains the mathematical models used in this paper. In this paper, a 7-DOF four-wheel vehicle

vertical model is used for the design of the active suspension controller that stabilises the vehicle during extreme driving condition. The performance of the designed controllers is then verified using 14-DOF full car nonlinear model, which is more close to the actual system. 14-DOF nonlinear car model allows taking into consideration nonlinear load transfer, the coupling effect between the vehicle suspension and the handling dynamics.

2.1. Vehicle mathematical model 14-DOF

Figure 1 exhibits the schematics of the 14-DOF vehicle model used to investigate the effects of the proposed controller. The nonlinear passive vehicle model as discussed by [20] includes 6-DOF at the mass centre of the vehicle body and 2-DOF at each of the four wheels. The 6-DOF represents the vehicle body longitudinal, lateral and vertical motions along with roll, pitch and yaw motions in x , y and z directions in body-fixed coordinate. The 2-DOF at each of the four wheels represents vertical and rotational motions of each wheel.

14-DOF model dynamics equations for vehicle bodys longitudinal, lateral and vertical motions along with roll, pitch and yaw motions in x , y and z directions in body-fixed coordinate can be rewritten as

$$m(\dot{u} + \omega_y w - \omega_z v) = \sum_{i,j=1}^4 F_{x_{sij}} + mg \sin \theta \quad (1)$$

$$m(\dot{v} + \omega_z u - \omega_x w) = \sum_{i,j=1}^4 F_{y_{sij}} - mg \sin \phi \cos \theta \quad (2)$$

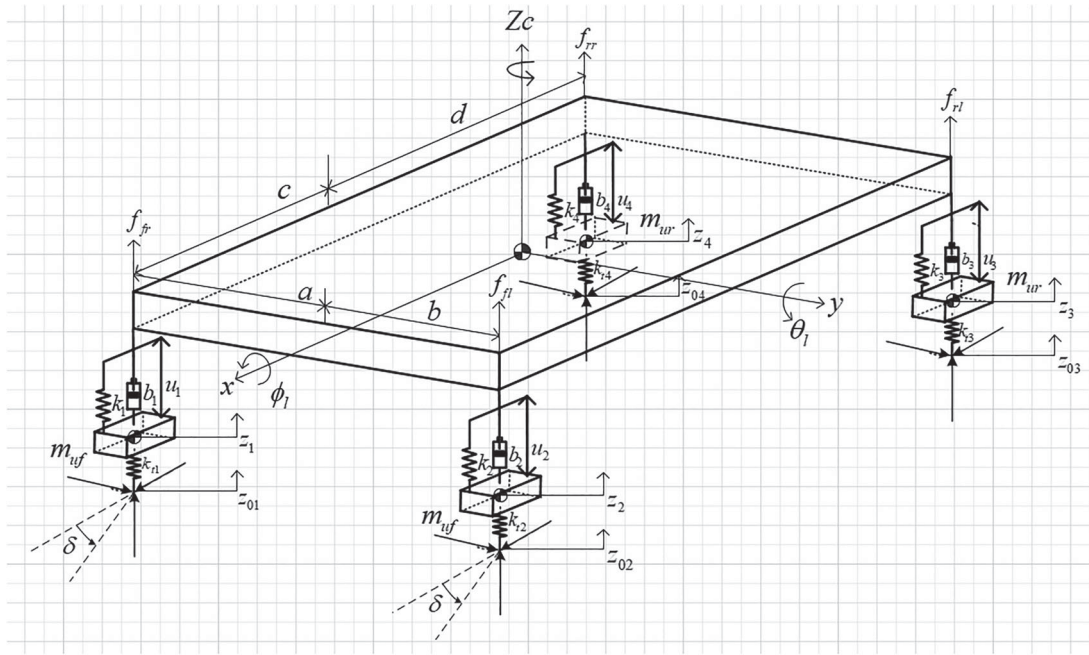


Figure 2. Simplified 7-DOF vehicle model for active suspension.

$$m(\dot{w} + \omega_x v - \omega_y u) = \sum_{i,j=1}^4 (F_{zsj} + F_{dzij}) - mg \cos \phi \cos \theta \quad (3)$$

$$J_x \dot{\omega}_x = \sum_{i,j=1}^4 M_{xij} + (F_{zslf} + F_{zslr})wr - (F_{zsrfl} + F_{zsrfr})wl \quad (4)$$

$$J_y \dot{\omega}_y = \sum_{i,j=1}^4 M_{yij} + (F_{zslr} + F_{zsrfr})lr - (F_{zsrfl} + F_{zslfl})lf \quad (5)$$

$$J_z \dot{\omega}_z = \sum_{i,j=1}^4 M_{zij} + (F_{xsrf} + F_{xsrr})wl - (F_{xslf} + F_{xslr})wr + (F_{ysrf} + F_{yslf})lf - (F_{ysrr} + F_{yslr})lr \quad (6)$$

In Equations (1), (2) and (3), m is the sprung mass and g is known as gravitational acceleration, u, v and w are the longitudinal, lateral and vertical velocities respectively, similarly the forces $F_{xsi}, F_{ysi}, F_{zsi}$ respectively represent longitudinal, lateral and vertical forces acting at the mounting point of the car body, where ij subscript represents left-front, right-front, left-rear and right-rear respectively throughout this paper. ω_x, ω_y and ω_z in Equations (4), (5) and (6) are the roll, pitch and yaw angular velocities, J_x, J_y, J_z are the roll, pitch and yaw inertia, and $M_{xij}, M_{yij}, M_{zij}$ define the moments in x, y and z directions respectively.

Also Equations for 2-DOF at each of the four wheels which represents vertical (w_{ui}) and rotational (ω_{wi}) motions of each wheel can be written as (7) and (8)

$$m_{ui}(\dot{w}_{ui} + \omega_x v_{ui} - \omega_y u_{ui}) = F_{zgsi}$$

$$- m_{ui}g \cos \theta_n \cos \phi_n - F_{zsi} - F_{dzi} \quad (7)$$

$$J_{wi} \dot{\omega}_{wi} = -F_{xwi} r_i + \tau_b \quad (8)$$

The cardan angles (θ, ϕ , and ψ) can be calculated using the following equations:

$$\dot{\theta} = \omega_y \cos \phi - \omega_z \sin \phi \quad (9)$$

$$\dot{\phi} = \omega_x + \omega_y \sin \phi \tan \theta + \omega_z \cos \phi \tan \theta \quad (10)$$

$$\dot{\psi} = \omega_y \frac{\sin \phi}{\cos \theta} + \omega_z \frac{\cos \phi}{\cos \theta} \quad (11)$$

2.2. Vehicle vertical mathematical model 7-DOF

To design a back-stepping controller, a 7-DOF simple linear full car model as presented in [11] is used which ignores the longitudinal, lateral and yaw motions of car body and rotational motion of wheel. In this full-car linear model, 3-DOF represents pitch, roll and heave motions of car body and 4-DOF represents vertical tire motion for each tire as shown in Figure 2.

Dynamics equations for the motions of car body and for the vertical motion of four tires are as follows:

$$m \ddot{z}_c = \sum_{i,j=1}^4 f_{ij} \quad (12)$$

$$J_x \ddot{\phi}_l = m(h+z)\dot{v} + (-f_{fr} + f_{fl})w_r + (-f_{rr} + f_{rl})w_l \quad (13)$$

$$J_y \ddot{\theta}_l = m(h+z)\dot{u} - (f_{fr} + f_{fl})l_f + (f_{rl} + f_{rr})l_r \quad (14)$$

$$m_{ui} \ddot{z}_{ij} = -k_{tij}(z_{ij} - z_{oij}) - f_{ij} \quad (15)$$

F_{ij} in Equation (12) defines the vertical forces transferred to the sprung mass in the vehicle body fixed frame. in Equation (13) h is the height of the centre

of gravity (c.g) of the car body from ground. For further simplification, Equations (13) and (14) can be written as

$$J_x \ddot{\phi}_l = m(h+z)\dot{v} + E_\phi \quad (16)$$

$$J_y \ddot{\theta}_l = m(h+z)\dot{u} + E_\theta \quad (17)$$

where E_ϕ and E_θ are the intermediate control variables and can be written as

$$E_\phi = (-f_{fr} + f_{fl})w_r + (-f_{rr} + f_{rl})w_l \quad (18)$$

$$E_\theta = -(f_{fr} + f_{fl})l_f + (f_{rl} + f_{rr})l_r \quad (19)$$

Suspension forces of car body are generated by the addition of actuators to the suspension system. This addition along with spring and dumper can produce upward and downward control forces, these forces can be calculated as

$$f_{fr} = k_{fr}(z_{fr} - z_c + l_f\theta_l + w_r\phi_l) + b_{fr}(\dot{z}_{fr} - \dot{z}_c + l_f\dot{\theta}_l + w_r\dot{\phi}_l) + u_{fr} \quad (20)$$

$$f_{fl} = k_{fl}(z_{fl} - z_c + l_f\theta_l - w_l\phi_l) + b_{fl}(\dot{z}_{fl} - \dot{z}_c + l_f\dot{\theta}_l - w_l\dot{\phi}_l) + u_{fl} \quad (21)$$

$$f_{rl} = k_{rl}(z_{rl} - z_c - l_r\theta_l - w_l\phi_l) + b_{rl}(\dot{z}_{rl} - \dot{z}_c - l_r\dot{\theta}_l - w_l\dot{\phi}_l) + u_{rl} \quad (22)$$

$$f_{rr} = k_{rr}(z_{rr} - z_c - l_r\theta_l + w_r\phi_l) + b_{rr}(\dot{z}_{rr} - \dot{z}_c - l_r\dot{\theta}_l + w_r\dot{\phi}_l) + u_{rr} \quad (23)$$

In Equations (20)–(23), $k_{fr}, k_{fl}, k_{rl}, k_{rr}$ represent spring stiffness, $b_{fr}, b_{fl}, b_{rl}, b_{rr}$ define damping coefficients, $z_{fr}, z_{fl}, z_{rl}, z_{rr}$ denote the vertical displacement and $u_{fr}, u_{fl}, u_{rl}, u_{rr}$ are called the control inputs at front right, front left, rear left and rear right respectively, similarly l_f, l_r is the distance from the centre of gravity to the front and rear axles. Using Equations (18) and (19), the intermediate control variables the suspension forces f_{ij} can be written as

$$\begin{bmatrix} E_\theta \\ E_\phi \end{bmatrix} = \begin{bmatrix} -w_r & w_r & -w_l & w_l \\ -l_f & -l_f & l_r & l_r \end{bmatrix} \begin{bmatrix} f_{fr} \\ f_{fl} \\ f_{rr} \\ f_{rl} \end{bmatrix} \quad (24)$$

where

$$A = \begin{bmatrix} -w_r & w_r & -w_l & w_l \\ -l_f & -l_f & l_r & l_r \end{bmatrix} \quad (25)$$

$$\begin{bmatrix} f_{fr} \\ f_{fl} \\ f_{rr} \\ f_{rl} \end{bmatrix} = A^{-1} \begin{bmatrix} E_\theta \\ E_\phi \end{bmatrix} \quad (26)$$

Since A is a rectangular matrix, therefore we can use the following matrix identity:

$$A^{-1} = (A^T * A)^{-1} A^T$$

$$\begin{bmatrix} f_{fr} \\ f_{fl} \\ f_{rr} \\ f_{rl} \end{bmatrix} = (A^T * A)^{-1} A^T \begin{bmatrix} E_\theta \\ E_\phi \end{bmatrix} \quad (27)$$

2.3. Nonlinear tyre model

Tyre model is one of the basic building blocks of every vehicle dynamic simulation. Tyre model produces the forces required to drive the simulation/model. Nonlinear tyre forces (F_{xij}, F_{yij}) which are used in the mentioned vehicle model are calculated as function of tyre slip using Pacejka's Magic Formula as explained by [21]. The total friction coefficient at each wheel is calculated as a function of total slip using magic formula as

$$\mu_{ij}(s_{ij}) = D \sin(C \arctan(Bs_{ij})) \quad (28)$$

where μ_{ij} is the friction coefficient, D is the peak value and C is the shape factor of tyre curve shown in Figure 3. The resultant tire slip (s_{ij}) is calculated as

$$s_{ij} = \sqrt{s_{xij}^2 + s_{yij}^2} \quad (29)$$

where (s_{xij}) are the theoretical longitudinal slips and (s_{yij}) are the lateral slips of the corresponding wheel. The longitudinal and the lateral slips are calculated as

$$s_{xij} = \frac{V_{xij} - \omega_{ij}r_{ij}}{\omega_{ij}r_{ij}} \quad (30)$$

$$s_{yij} = \frac{V_{yij}}{\omega_{ij}r_{ij}} = (1 + s_{xij}) \tan(\alpha_{ij}) \quad (31)$$

where (ω_{ij}) is the rotational speed of each of the four wheels, (r_{ij}) is the radius of the corresponding wheel and (V_{xij}, V_{yij}) are the longitudinal and lateral components of the vehicle body velocity vector at the corresponding wheels. The slip angle at each wheel is calculated as

$$\tan(\alpha_{ij}) = \frac{V_{yij}}{V_{xij}} \quad (32)$$

Using the friction circle equation, the friction coefficient components in the longitudinal and lateral direction are given as

$$\mu_{xij} = -\frac{s_{xij}}{s_{ij}} \mu_{ij}(s_{ij}) \quad (33)$$

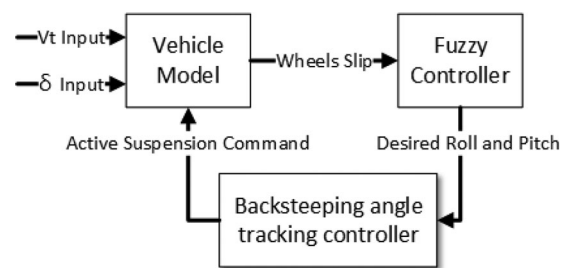


Figure 3. Magic formula [21] slip ratio versus friction coefficient.

$$\mu_{yij} = -\frac{s_{yij}}{s_{ij}} \mu_{ij}(s_{ij}) \quad (34)$$

Using (F_{zij}) as the vertical force on each of the four wheels, the longitudinal and lateral tyre forces can be calculated as s

$$F_{xij} = \mu_{xij} F_{zij}, \quad F_{yij} = \mu_{yij} F_{zij} \quad (35)$$

3. Control design

This section discusses the design of the controllers used for the proposed ASCS. Figure 4 shows the main block diagram for the designed control system. The ASCS will be implemented in two stages. In first stage, based on the slipping condition of the individual wheels a fuzzy controller is used to calculate the desired roll and pitch angle of the vehicle to minimise the slip of the individual wheel. In the second stage, based on the inputs from the fuzzy controller, a backstepping controller is used to generate the control inputs for the individual suspension in order to increase the vertical load on the slipping wheels. The details of the individual controller are explained in the following section.

3.1. Fuzzy controller

The dynamic nature of the vehicles with uncertain and some time imprecise sensor information makes it very difficult to accurately and completely model the environment of the vehicle [22]. The tyre models and vehicle system dynamics are complex and non-linear, and the interaction between the wheels and the ground is hard to model, which led us to design a fuzzy controller for the calculation of desired pitch and roll angles using slip information, i.e. a control system based upon fuzzy logic [23]. The tyre model shown in Figure 3 is approximated using the nonlinear sigmoid and a triangular membership function. The fuzzy control does not need a complete mathematical model of the controlled system. One of the first fuzzy controllers was proposed in [24]. Since then, fuzzy control has been applied to many problems for the control of car-like vehicles [25–27].

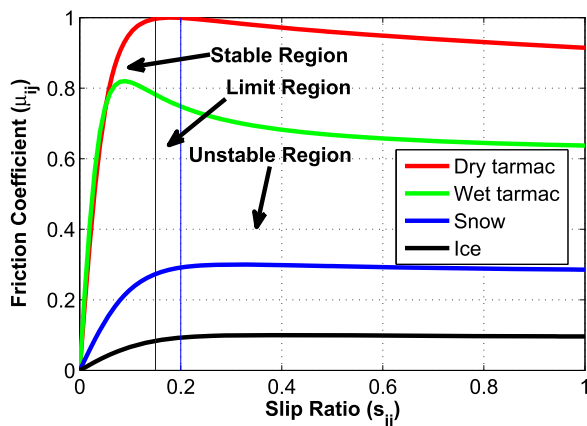


Figure 4. Control architecture for slipping control.

In this paper due to the complexity of the tyre models and the difficulty to model the interaction between the wheels and the ground, the fuzzy controller is used to generate the desired roll and pitch angle based on the slip ratio of the individual wheels. Figure 3 shows the plots of Magic formula as explained by Section 2.3 for different road conditions. Based on Figure 3, the relationship between friction and slip can be divided into three regions: a stable or always controllable region, a limit region or partially controllable region, and an unstable or uncontrollable region. In the stable region, the tyre road offers maximum friction forces and the vehicle is controllable. As the slip ratio increases to the limit region, the forces provided by the tyre road interaction reach its peak value, which restricts the maximum driving force. If the slip ratio keeps increasing, it will enter the unstable region where the friction forces saturate and reach its maximum value, the further increase in slip ratio will have no effects on the available friction forces, in this region due to the limited friction forces the vehicle could become unstable and uncontrollable.

Based on the slip information from the individual wheels of the vehicle, the fuzzy controller will generate roll and pitch angles required to increase the vertical load on slipping wheels. To implement the relationship between the slips of the individual wheels and the required roll and pitch angles, the fuzzy values of each input variable in the form of individual wheel slip are described as stable slip region (s_{ijs}), limit slip region (s_{ijl}) and zero slip (ZS). The input membership functions for s_{ij} are shown in Figure 5.

In this figure, the membership functions are chosen based on the stability regions defined in Figure 3. The fuzzy controller is designed to produce linear output in the stable region because of the maximum available friction while a sigmoid function is selected for the limit region. The fuzzy controller will maintain its maximum output value for the slip inputs corresponding to the unstable region.

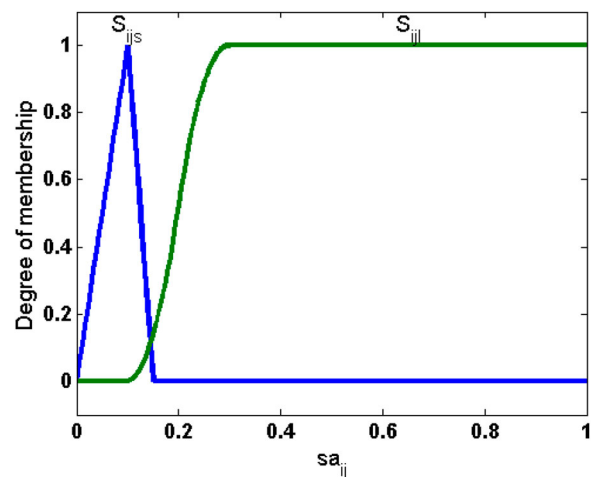


Figure 5. Membership functions for input s_{ij} calculation.

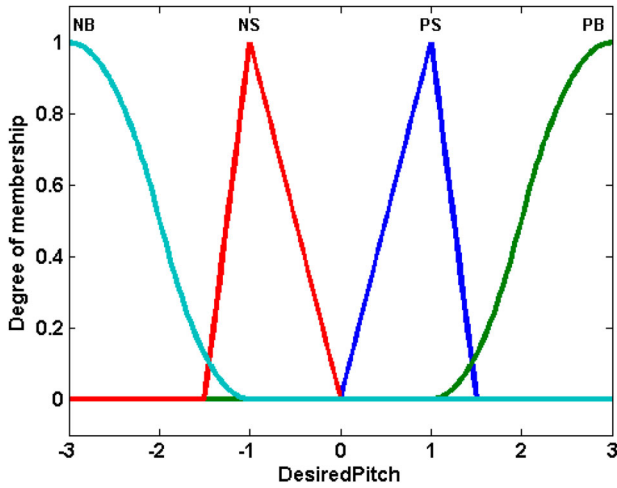


Figure 6. Membership functions for desired pitch calculation.

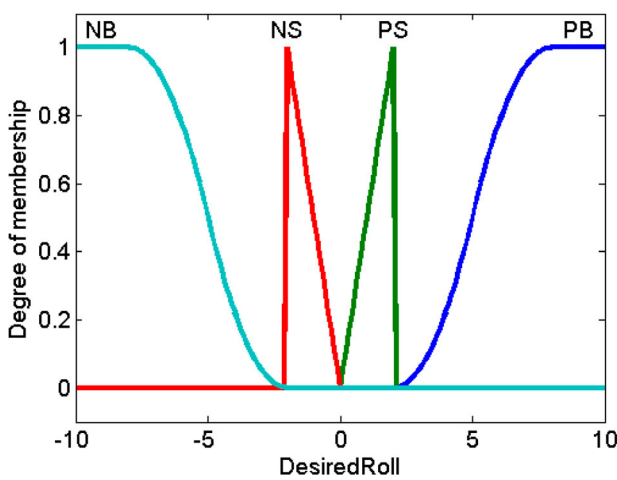


Figure 7. Membership functions for desired roll calculation.

In this research, the output pitch and roll variables are described as Positive Big (PB), Positive Small (PS), Zero (Z), Negative Small (NS), and Negative Big (NB). Based on the stability regions, the output membership function is chosen to produce small output in the stable region and to make the fuzzy controller most active in the limit region. The fuzzy controller maximum output for desired pitch angle is limited to three degree while the roll angle maximum output is limited to 10 degree due to active suspension limitations [19]. The output membership function of the designed controller for pitch calculation is shown in Figure 6, while output membership function for roll calculation is shown in Figure 7. After the formulation of the fuzzy rules, the characteristic graph of the presented fuzzy controller can be as shown in Figure 8. Based on the above discussion, the fuzzy rules are summarized in Table 1.

3.2. Back-stepping controller

In this paper, an iterative back-stepping nonlinear control technique is utilized to design a roll and pitch tracking controller which is robust as compared to other

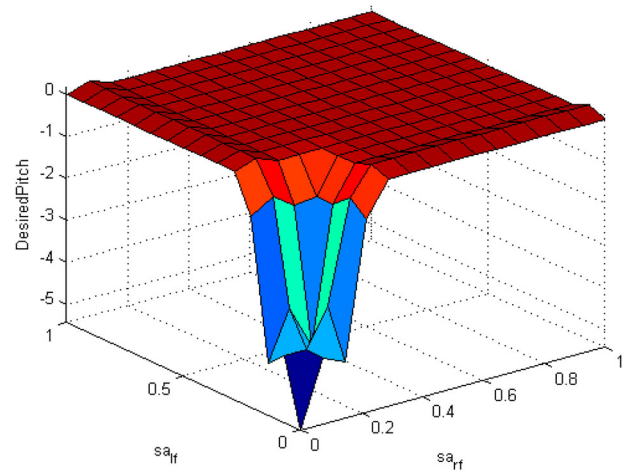


Figure 8. The characteristic graph for fuzzy logic.

Table 1. Fuzzy controller rules for active slip control.

Inputs				Outputs	
S_{rf}	S_{lf}	S_{lr}	S_{rr}	Pitch	Roll
S_{rfs}	ZS	ZS	ZS	PS	PS
ZS	S_{lfs}	ZS	ZS	PS	NS
ZS	ZS	S_{lrs}	ZS	NS	NS
ZS	ZS	ZS	S_{lrrs}	NS	PS
S_{rfl}	ZS	ZS	ZS	PB	PB
ZS	S_{lfl}	ZS	ZS	PB	NB
ZS	ZS	S_{lrl}	ZS	NB	NB
ZS	ZS	ZS	S_{lrrl}	NB	PB
S_{rfs}	S_{lfs}	ZS	ZS	PS	Z
ZS	ZS	S_{lrs}	S_{lrrs}	NS	Z
S_{rfs}	ZS	ZS	S_{lrrs}	Z	PS
ZS	S_{lfs}	S_{lrs}	ZS	Z	NS
S_{rfl}	S_{lfl}	ZS	ZS	PB	Z
ZS	ZS	S_{lrl}	S_{lrrl}	NB	Z
S_{rfl}	ZS	ZS	S_{lrrl}	Z	PB
ZS	S_{lfl}	S_{lrl}	ZS	Z	NB
S_{rfs}	S_{lfl}	S_{lrl}	S_{lrrl}	NB	NB
S_{rfl}	S_{lfs}	S_{lrl}	S_{lrrl}	NB	PB
S_{rfl}	S_{lfl}	S_{lrs}	S_{lrrl}	PB	PB
S_{rfl}	S_{lfl}	S_{lrl}	S_{lrrs}	PB	NB
S_{rfl}	S_{lfs}	S_{lrs}	S_{lrrs}	PB	PB
S_{rfs}	S_{lfl}	S_{lrs}	S_{lrrs}	PB	NB
S_{rfs}	S_{lfs}	S_{lrl}	S_{lrrs}	NB	NB
S_{rfs}	S_{lfs}	S_{lrs}	S_{lrrl}	NB	PB
S_{rfs}	S_{lfl}	S_{lrl}	S_{lrrs}	Z	NB
S_{rfl}	S_{lfs}	S_{lrs}	S_{lrrl}	Z	PB

linear control techniques [28]. This controller will generate the desired roll and pitch angle commanded by fuzzy controller using active suspension of the vehicle. The backstepping controller plays an important role in incremental stability where the uniform asymptotic stability of every trajectory is required rather than that of equilibrium points or in case of time varying trajectory [29]. The back-stepping controller is an effective approach against disturbances and can avoid unwanted cancellation. The controller design procedure involves n -steps, and a virtual controller is designed in each step to stabilize the corresponding subsystem. Each subsystem is defined in terms of the errors between the output of the actual system and the desired state.

$$\eta_1 = \theta - \theta_{des} \quad (36)$$

$$\eta_2 = \dot{\theta} - \dot{\zeta}_1 \quad (37)$$

where θ_{des} is the desired pitch angle to be tracked and ζ_1 is the virtual controller to minimize η_1 . The following Lyapunov candidate function is used to get the required virtual controller.

$$V_1 = \frac{1}{2}\eta_1^2 \quad (38)$$

$$\dot{V}_1 = \eta_1 \dot{\eta}_1 \quad (39)$$

Differentiating Equation (36) and using Equation (37), we get

$$\dot{\eta}_1 = \eta_2 + \zeta_1 - \dot{\theta}_{des} \quad (40)$$

Now putting Equation (40) in (39) as

$$\dot{V}_1 = \eta_1 \eta_2 + \eta_1 (\zeta_1 - \dot{\theta}_{des}) \quad (41)$$

For the global asymptotic stability, \dot{V}_1 needs to be negative definite for all $(\eta_1, \eta_2) \neq 0$. We choose the stabilizing function ζ_1 as

$$\zeta_1 = -\kappa_1 \eta_1 + \dot{\theta}_{des} \quad (42)$$

substituting stabilizing function ζ_1 into Equation (41), we can get the following equation:

$$\dot{V}_1 = \eta_1 \eta_2 - \kappa_1 \eta_1^2 \quad (43)$$

From Equation (43), we can say that the derivative of the Lyapunov function is not negative definite so the stability of the system cannot be ensured. Therefore another Lyapunov function is needed to get the final controller which can stabilize the system. The second Lyapunov function is selected as

$$V_2 = V_1 + \frac{1}{2}\eta_2^2 \quad (44)$$

Differentiating the above equation and by using Equations (37),(42) and (43) we can get

$$\dot{V}_2 = (\eta_1 \eta_2 - \kappa_1 \eta_1^2) + \eta_2 (\dot{\eta}_2 - \dot{\zeta}_1) \quad (45)$$

Using definition of Equation (17), the intermediate control variable E_θ is derived as

$$E_\theta = -(h+z)\dot{u} + J_y(\dot{\zeta}_1 - \eta_1 - \kappa_2 \eta_2) \quad (46)$$

which will ensure the negative definiteness of newly selected Lyapunov function as shown below.

$$\dot{V}_2 = -\kappa_1 \eta_1^2 - \kappa_2 \eta_2^2 < 0 \quad \forall \eta_1, \eta_2 \neq 0 \quad (47)$$

where κ_1 and κ_2 are two Hurwitz constants.

Similarly following the same procedure, we can construct the controllers for the roll motions of the vehicle body given in the following equations:

$$E_\phi = -(h+z)\dot{v} + J_x(\dot{\zeta}_3 - \eta_3 - \kappa_4 \eta_4) \quad (48)$$

Finally by substituting Equations (46) and (48) into Equation (27) and solving for u_{ij} , the control outputs can be derived as

$$u_{fr} = f_{fr} - k_1(z_1 - z_c + l_f \theta_l + w_r \phi_l) \quad (49)$$

Table 2. Vehicle and tyre parameters.

Variable	Data	Variable	Data
m(kg)	850	h(m)	0.5
J_z (kgm ²)	1400	J_w (kgm ²)	0.6
l _f (m)	1.5	l _r (m)	0.9
r_{ij} (m)	0.311	B-icy	4
C-icy	1.3	D-icy	0.6
C_{xij}	10000	C_{yij}	15000
B-dry	10	C-dry	1.9
D-dry	1.0	—	—

$$-b_1(\dot{z}_1 - \dot{z}_c + l_f \dot{\theta}_l + w_r \dot{\phi}_l) \quad (50)$$

$$u_{fl} = f_{fl} - k_2(z_2 - z_c + l_f \theta_l - w_l \phi_l) \quad (51)$$

$$-b_2(\dot{z}_2 - \dot{z}_c + l_f \dot{\theta}_l - w_l \dot{\phi}_l) \quad (52)$$

$$u_{rr} = f_{rr} - k_3(z_3 - z_c - l_r \theta_l - w_l \phi_l) \quad (53)$$

$$-b_3(\dot{z}_3 - \dot{z}_c - l_r \dot{\theta}_l - w_l \dot{\phi}_l) \quad (54)$$

$$u_{rl} = f_{rl} - k_4(z_4 - z_c - l_r \theta_l + w_r \phi_l) \quad (55)$$

$$-b_4(\dot{z}_4 - \dot{z}_c - l_r \dot{\theta}_l + w_r \dot{\phi}_l) \quad (56)$$

4. Simulations

In this section, two simulation scenarios corresponding to the driving manoeuvres of lane change and J-turn are considered with vehicle velocity of 22.2 and 10.2 m/s respectively. In the presented scenarios, the lane change scenario corresponds to high speed driving with small steering angle input while the J-turn corresponds to slow moving vehicle with high steering angle input. In both scenarios, the main control objective is to show the effectiveness of the presented controller by setting the road conditions for the left-front and left-rear to be dry and the road conditions for the right-front and right-rear to be icy road. Both simulations are performed using the high-fidelity nonlinear vehicle model with nonlinear tyre dynamics. The vehicle and tyre model parameters are listed in Table 2.

4.1. Lane change manoeuvres

In the first scenario, a lane change scenario is simulated using a fast moving vehicle with small steering angle. For this scenario, the simulation is initialized with the actual driver inputs corresponding to the 22.2m/s vehicle total velocity and steering angle input profile as shown in Figure 9. In this scenario, the control objective is to track desired yaw rate in slippery conditions by minimising the required tire friction using fuzzy and backstepping controller with the help of the active suspension of the vehicle. The corresponding desired and actual trajectories generated are shown in Figure 10. From the generated trajectories, one can see that in the simulated scenario the vehicle becomes unstable without the use of controller, and this is due to the limited friction force on slippery road.

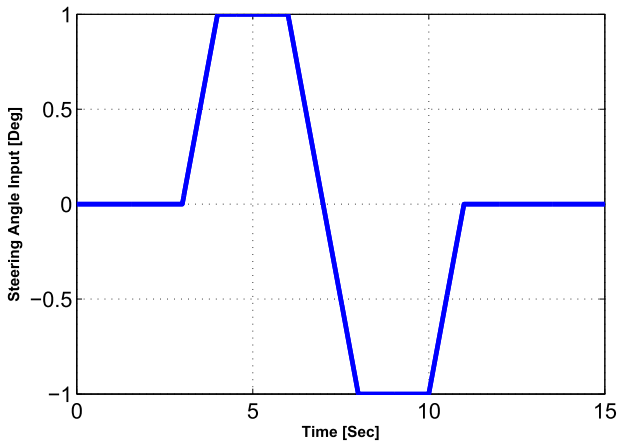


Figure 9. Steering angle input for lane-change simulation.

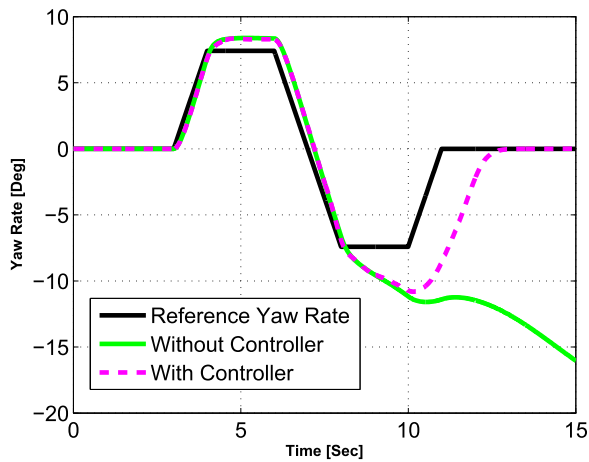


Figure 10. Yaw Rate comparison for lane-change simulation.

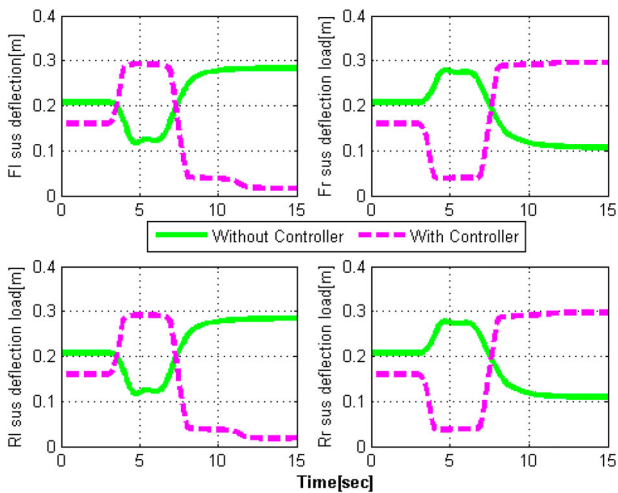


Figure 11. Suspension deflection for lane-change simulation.

Figure 11 shows the comparison of the suspension deflection generated with and without controller. It can be seen that suspension is more active with controller case, and the suspension is deflected in opposite direction in order to redistribute the vehicle weight according to the wheel slips. Figure 12 shows the required friction coefficient of each wheel, without controller the

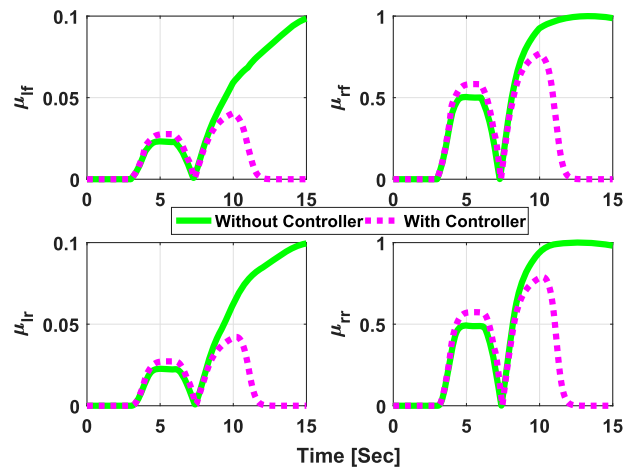


Figure 12. Friction coefficient for lane-change simulation.

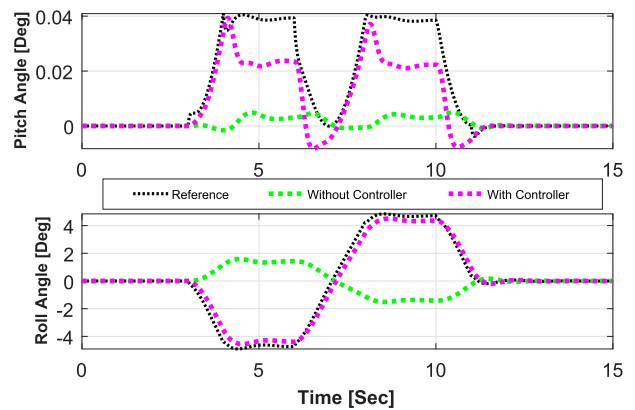


Figure 13. Roll and pitch angles (fuzzy controller and actual) for J-Turn simulation.

friction coefficients saturate because of slippery conditions.

4.2. J-Turn manoeuvres

In the second scenario, a J-turn manoeuvre scenario is simulated using a slow moving vehicle with large

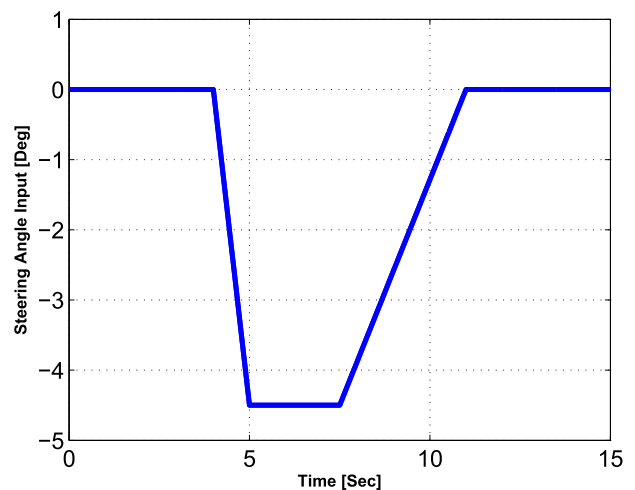


Figure 14. Steering angle input for J-Turn simulation.

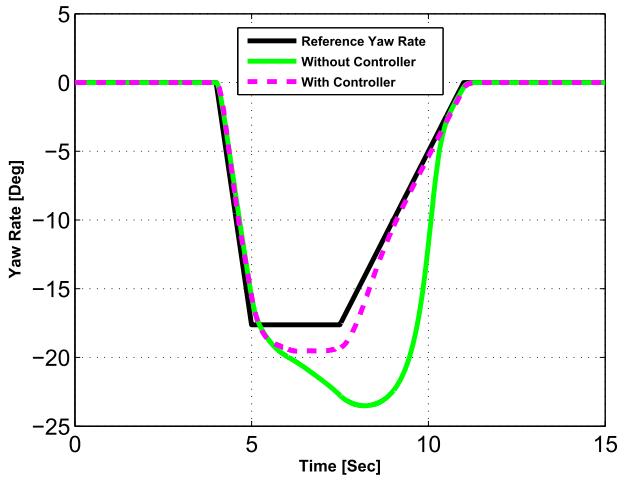


Figure 15. Yaw rate comparison for J-Turn simulation.

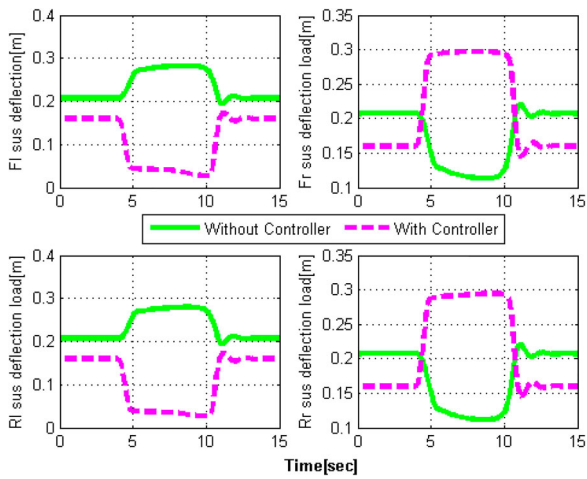


Figure 16. Suspension deflection for J-Turn simulation.

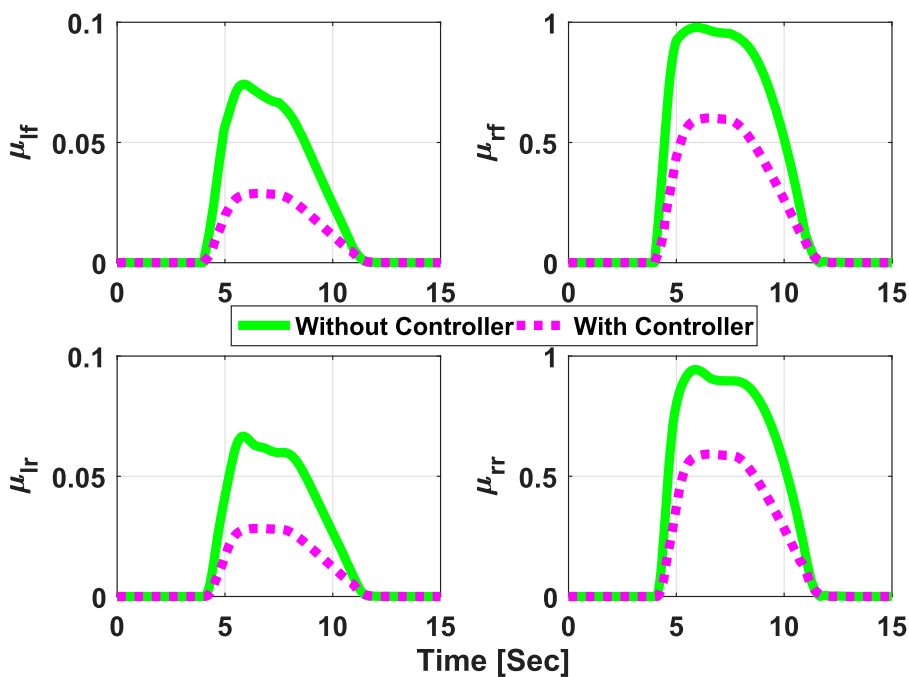


Figure 17. Friction coefficient for J-Turn simulation.

steering angle. For this scenario, the simulation is initialized with the actual driver inputs corresponding to the 10.2 m/s vehicle total velocity and steering angle input profile as shown in Figure 14. In this scenario, similar results were observed as of lane change scenario, the yaw rate tracking is improved as shown in Figure 15.

The comparison of the suspension deflection generated with and without controller is shown in Figure 16 while Figure 17 shows the required friction coefficient of each wheel. It can be seen that the required friction coefficients are reduced with the help of the presented controller. Figure 18 shows the comparison of the output of the fuzzy controller to the actual generated pitch and roll angles. From this figure, it can be seen that the controller actually tilts the vehicle in the opposite direction of motion using the active suspensions of the vehicle.

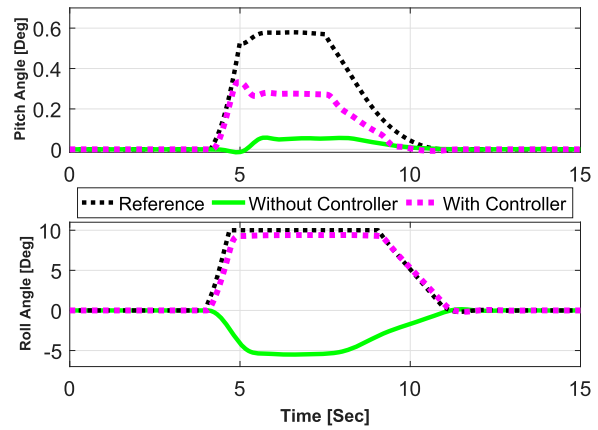


Figure 18. Roll and pitch angles (fuzzy controller and actual) for J-Turn simulation.

5. Conclusion

This paper presents an active slip control system using an active suspension of the vehicle. The integrated control mechanism is designed using a combination of a fuzzy controller and a nonlinear back-stepping controller to control the slip of the individual wheels with the help of the active suspension of the vehicle. The presented control mechanism is implemented in two steps. In the first step, based on the friction coefficient calculated from a nonlinear tyre model the fuzzy controller will generate the required pitch and roll angle needed to reduce the slipping by changing the vertical load of the individual wheel. In the second step, a nonlinear back-stepping controller is used to track the desired pitch and roll angle using the active suspension of the vehicle. The active suspension is used to manipulate the vertical load on the individual wheel to reduce the slip of the individual wheel. Two simulation scenarios, a J-turn and a lane-change manoeuvre, were considered to check the effectiveness of the presented controller. The simulation results using a high-fidelity vehicle model under different driving conditions indicate that the proposed system can significantly improve the vehicle performance by tracking the reference trajectory and reducing the slipping of the individual wheel.

Acknowledgments

This study was supported by the BK-21 Plus Program funded by the Ministry of Education and National Research Foundation of South Korea (NRF).

Disclosure statement

No potential conflict of interest was reported by the author(s).

Funding

This study was supported by the BK-21 Plus Program funded by the Ministry of Education and National Research Foundation of South Korea (NRF).

References

- [1] Chen Y, Li L. *Advances in intelligent vehicles*. Intelligent Systems Series. Boston: Academic Press; 2014.
- [2] De Santiago J, Bernhoff H, Ekergerd B, et al. Electrical motor drivelines in commercial all-electric vehicles: A review. *IEEE Transactions on Vehicular Technology*. 2012;61(2):475–484.
- [3] Wang J, Wang R, Jing H, Chen N. Coordinated active steering and four-wheel independently driving/braking control with control allocation. *Asian J Control*. 2016;18(1):98–111.
- [4] Li Q, Yu X-l, Zhang H, et al. Study on differential assist steering system with double in-wheel motors with intelligent controller. *Mathematical Problems in Engineering*. 2015;2015:1–8.
- [5] Zhang H, Zhang X, Wang J. Robust gain-scheduling energy-to-peak control of vehicle lateral dynamics stabilisation. *Vehicle System Dynamics*. 2014;52(3):309–340.
- [6] Prem P, Sivaraman P, S. Raj JSS, Sathik MJ, Almakhlles D. Fast charging converter and control algorithm for solar pv battery and electrical grid integrated electric vehicle charging station. *Automatika*. 2020;61(4):614–625.
- [7] Wang R, Wang J. Fault-tolerant control for electric ground vehicles with independently-actuated in-wheel motors. *J Dyn Syst Meas Control*. 2012;134(2):021014.
- [8] Perez-Pinal FJ, Cervantes I, Emadi A. Stability of an electric differential for traction applications. *IEEE Trans Vehicul Technol*. 2009;58(7):3224–3233.
- [9] Ahmad E, Iqbal J, Arshad Khan M, Liang W, Youn I. Predictive control using active aerodynamic surfaces to improve ride quality of a vehicle. *Electronics*. 2020;9(9):1463.
- [10] Shibahata Y, Shimada K, Tomari T. Improvement of vehicle maneuverability by direct yaw moment control. *Vehicle System Dynamics*. 1993;22(5-6):465–481.
- [11] Youn I, Youn E, Khan MA, Wu L, Tomizuka M. Combined effect of electronic stability control and active tilting control based on full-car nonlinear model. *The Dynamics of Vehicles on Roads and Tracks: Proceedings of the 24th Symposium of the International Association for Vehicle System Dynamics (IAVSD 2015)*; 2015 August 17–21; Graz, Austria. CRC Press; 2016, p. 345.
- [12] Chen B-C, Peng H. Differential-braking-based rollover prevention for sport utility vehicles with human-in-the-loop evaluations. *Vehicle System Dynamics*. 2001;36(4-5):359–389.
- [13] Tchamna R, Youn E, Youn I. Combined control effects of brake and active suspension control on the global safety of a full-car nonlinear model. *Vehicle System Dynamics*. 2014;52(1):69–91.
- [14] Lakehal-Ayat M, Diop S, Fenaux E. An improved active suspension yaw rate control. *Proceedings of the 2002 American Control Conference*, vol. 2. IEEE; 2002, p. 863–868.
- [15] March C, Shim T. Integrated control of suspension and front steering to enhance vehicle handling. *Proceedings of the Instit Mech Eng D J Automobile Eng*. 2007;221(4):377–391.
- [16] Liang W, Ahmac E, Khan MA, Youn I. Integration of active tilting control and full-wheel steering control system on vehicle lateral performance. *Int J Automotive Technol*. 2021;22(4):979–992.
- [17] Youn I. Optimal control of semi-active automobile suspension including preview information; 1994.
- [18] Youn I, Im J, Tomizuka M. Level and attitude control of the active suspension system with integral and derivative action. *Vehicle SystDynam*. 2006;44(9):659–674.
- [19] Youn I, Wu L, Youn E, Tomizuka M. Attitude motion control of the active suspension system with tracking controller. *Int J Automotive Technol*. 2015;16(4):593–601.
- [20] Shim T, Ghike C. Understanding the limitations of different vehicle models for roll dynamics studies. *Vehicle Syst Dynam*. 2007;45(3):191–216.
- [21] Bakker E, Nyborg L, Pacejka HB. Tyre modelling for use in vehicle dynamics studies. *SAE Technical Paper*, Tech. Rep., 1987.
- [22] Fraichard T, Garnier P. Fuzzy control to drive car-like vehicles. *Rob Auton Syst*. 2001;34(1):1–22.
- [23] Zadeh LA. Fuzzy sets. *Fuzzy Sets, Fuzzy Logic, And Fuzzy Systems: Selected Papers by Lotfi A Zadeh*. World Scientific; 1996, p. 394–432.

- [24] Mamdani EH. Application of fuzzy algorithms for control of simple dynamic plant. Proceedings of the Institution of Electrical Engineers, vol. 121, no. 12. IET; 1974. p. 1585–1588.
- [25] Pin FG, Watanabe Y. Steps toward sensor-based vehicle navigation in outdoor environments using a fuzzy behaviorist approach. *J Intelligent Fuzzy Syst.* 1993;1(2): 95–107.
- [26] Sugeno M. An experimental study on fuzzy parking control using a model car. *Industrial Applications of Fuzzy Control*; 1985.
- [27] Tanaka K, Sano M. Trajectory stabilization of a model car via fuzzy control. *Fuzzy Sets Syst.* 1995;70 (2-3):155–170.
- [28] Khan O, Pervaiz M, Ahmad E, Iqbal J. On the derivation of novel model and sophisticated control of flexible joint manipulator. *Rev Roumaine Sci Techn Electrotech Energ.* 2017;62(1):103–108.
- [29] Zamani M, van de Wouw N, Majumdar R. Backstepping controller synthesis and characterizations of incremental stability. *Syst Control Lett.* 2013;62(10): 949–962.